JOURNAL OF AIRCRAFT
Vol. 41, No. 4, July–August 2004

Dynamics and Control of Shock Motion in a Near-Isentropic Inlet

Douglas G. MacMartin*
California Institute of Technology, Pasadena, California 91125

Inlet pressure recovery of supersonic aircraft could be improved using a near-isentropic inlet with only a weak normal shock aft of the throat; however, such an inlet is highly susceptible to unstart. Small perturbations can move the shock ahead of the throat, where it is unstable. The dynamics of the inlet and shock are analyzed using a low-order model that captures both the nonlinear shock motion and inlet acoustic propagation. This model allows parametric exploration of both the potential and limitations of using control to stabilize actively the shock, including actuator authority as a function of location, actuator authority, and bandwidth requirements, and sensor requirements. A simple control law is shown to be sufficient to stabilize the shock motion.

I. Introduction

INLETS for supersonic aircraft decelerate the incoming flow to the desired (typically) subsonic condition, recovering the energy as pressure. Unless the throat Mach number is exactly one, there will be a terminal shock aft of the diffuser throat that introduces losses. A weak shock results in lower loss, but is more susceptible to disturbances. If the perturbed shock moves ahead of the throat, it becomes unstable, leading to inlet unstart.[1–4] Active control of the inlet and shock could enable operation closer to the stability boundary, yielding higher inlet pressure recovery. This paper describes low-order modeling of the inlet/shock dynamics and investigates active control based on this model. A schematic of a hypothetical inlet is shown in Fig. 1, illustrating the area variation, Mach number variation, nominal shock location, and disturbances.

The shock responds to both upstream (atmospheric) and downstream (compressor) disturbances, leading to unstart if the shock moves past the throat. Atmospheric disturbances can also lead to unstart if the throat Mach number drops below unity; a new (unstable) shock will form immediately upstream.[1] Thus, control of inlet unstart requires both control of the existing terminal shock and control of the throat Mach number; although both are considered herein, the primary focus is on the former problem. The control architecture explored uses variable bleed as an actuator and considers both feedforward control of disturbances and feedback control; the former is required because of the propagation time delays and the latter to compensate for uncertainty.

A low-order model that captures the key features of the shock response is invaluable in the development of control strategies. When quasi-one-dimensional flow is assumed, a single nonlinear ordinary differential equation (ODE) captures the shock motion. The approach is based on that used by Hurrell[5] to investigate shock motion and by Culick and Rogers[6] and Yang and Culick[7] to analyze the acoustic reflection and transmission properties of a normal shock. In these papers, the response to pressure disturbances at the shock is computed by perturbing the shock equations and taking terms to first order. This linearization approach is extended here by explicitly representing the upstream and downstream perturbations as acoustic and entropy waves. The model captures both the nonlinear shock motion and the downstream propagating acoustic wave that results. The propagation of disturbances through the inlet is based on perturbation of the Euler equations. Reflection off the downstream compressor boundary condition is also required to capture the full system behavior. Viscous and three-dimensional effects are not included in this reduced-order model although these are clearly relevant to a detailed description of unstart, for example, see Zha et. al.[4]

In this paper, first the inlet/shock system dynamics is derived. This model is then used to evaluate the potential for active control to stabilize the shock location actively. The following topics are addressed parametrically: 1) the open-loop domain of attraction of the existing shock, as a function of disturbance bandwidth and amplitude, and the qualitative response of the shock to disturbances; 2) the actuator and sensor location; 3) the actuator bandwidth and authority requirements; and 4) the control algorithm.

The shock location can be stabilized using a simple controller requiring feedback of a single shock location sensor to downstream bleed.

II. Modeling Approach and Assumptions

Assume quasi-one-dimensional flow, and consider perturbations about a nominal flow that can be reasonably approximated by isentropic flow away from the terminal normal shock. Perturbations can be represented as the sum of three waves, two acoustic and entropy, traveling at $(1 + M)$, $(1 - M)$, and M times the speed of sound, respectively. In the subsonic regime, the acoustic waves propagate upstream and downstream; in the supersonic regime both travel downstream and will be referred to as fast and slow waves, respectively. The propagation time and variation in amplitude with changing cross-sectional area of the inlet can be obtained by expanding the Euler equations about the nominal solution. The shock motion and the downstream propagating acoustic wave are computed in response to all of the disturbances via perturbations of the usual shock equations. The assumptions are similar to those in Ref. 6; the derivation is extended to capture all of the disturbances. This permits more general treatment of the dynamics and the reflection and transmission coefficients.

The assumptions are as follows:

1) Only quasi-one-dimensional flow is considered; in particular, there is neither communication through the boundary layer nor shock–boundary-layer interaction, and actuation is assumed to affect the bulk flow immediately.

2) No additional shocks are considered explicitly; however, perturbations in the throat Mach number that would lead to a new shock are captured.

3) The shock satisfies quasi-steady shock equations at each instant of time.[6]

4) The unperturbed flow close to the shock location is isentropic both upstream and downstream. The propagation of disturbances through the inlet is only captured accurately if the unperturbed flow is everywhere isentropic (except across the shock).

5) Propagation of disturbances is nondispersive; changes in the shape of the waveform due to amplitude-dependent propagation speed is not captured.

Received 4 January 2003; revision received 30 April 2003; accepted for publication 1 May 2003. Copyright © 2003 by the American Institute of Aeronautics and Astronautics, Inc. All rights reserved. Copies of this paper may be made for personal or internal use, on condition that the copier pay the $10.00 per-copy fee to the Copyright Clearance Center, Inc., 222 Rosewood Drive, Danvers, MA 01923; include the code 0021-8669/04 $10.00 in correspondence with the CCC.

*Senior Research Fellow, Department of Control and Dynamical Systems; macmardg@cds.caltech.edu. Senior Member AIAA.

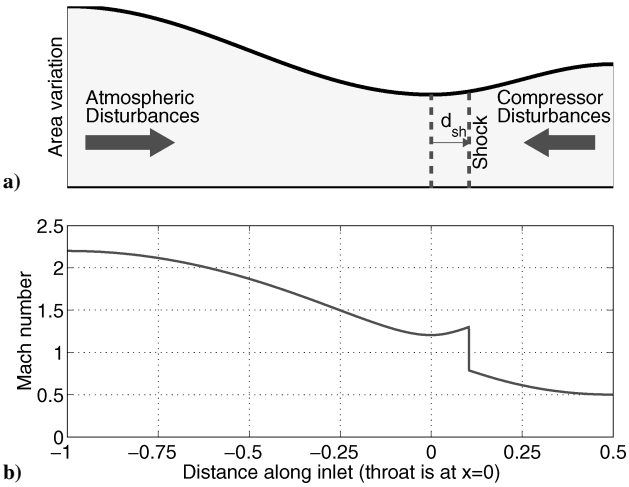

Fig. 1 Hypothetical near-isentropic inlet, with $M_{\text{th}} = 1.2$ and $M_{\text{sh}} = 1.3$; system perturbed both by upstream (atmospheric) and downstream (compressor) disturbances: a) area variation and b) corresponding Mach number.

The resulting equations can be further simplified for a weak shock by taking terms only to first order in $M_1 - 1$.

The cosine area variation shown in Fig. 1 will be used to illustrate behavior for a specific inlet geometry. With inlet Mach number $M_\infty = 2.2$, this leads to a throat Mach number $M_{\text{th}} = 1.2$. The shock is set at $M_{\text{sh}} = 1.3$, and the exit (compressor) Mach number is $M_c = 0.5$.

III. Shock Dynamics

The derivation follows from three sets of equations: 1) the usual shock equations, in the frame of reference of the moving shock (and, thus, dependent on the velocity of the shock); 2) the isentropic relationships, which give the variation in the nominal upstream and downstream flow variables as a function of the area variation, which is in turn a function of the shock location; and 3) the relationships between perturbations in the upstream and downstream flow variables and the upstream and downstream propagating waves.

The upstream variables denoted by subscript 1, and downstream variables, denoted by subscript 2, are related by the usual shock equations, in the frame of reference of the moving shock:

$$p_2/p_1 = 1 + [2\gamma/(\gamma+1)]\left(M_1^2 - 1\right) \tag{1}$$

$$u_2/u_1 = 1 - [2/(\gamma+1)]\left[\left(M_1^2 - 1\right)/M_1^2\right] \tag{2}$$

and $(M_2/M_1)^2 = (u_2/u_1)(p_2/p_1)^{-1}$. The nominal isentropic flow conditions that the shock moves into (in the inlet frame of reference), denoted by an overbar satisfy

$$\frac{1}{M^2-1}\left(\frac{1}{A}\frac{\mathrm{d}A}{\mathrm{d}x}\right) = \frac{1}{u}\frac{\partial u}{\partial x} \tag{3}$$

$$\frac{1}{M^2-1}\left(\frac{1}{A}\frac{\mathrm{d}A}{\mathrm{d}x}\right) = -\frac{1}{\gamma M^2}\left(\frac{1}{p}\frac{\partial p}{\partial x}\right) \tag{4}$$

$$\frac{1}{M^2-1}\left(\frac{1}{A}\frac{\mathrm{d}A}{\mathrm{d}x}\right) = \frac{2}{(\gamma-1)M^2+2}\left(\frac{1}{M}\frac{\partial M}{\partial x}\right) \tag{5}$$

The pressure immediately upstream of the shock for small shock motion ξ about a nominal location x_{sh} is $p_1(x_0+\xi) = \bar{p}_1(x_0) + p_1'(\xi)$, where

$$p_1'(\xi) = \frac{\partial \bar{p}_1}{\partial x}\xi + \delta p_1 \tag{6}$$

The perturbation in the Mach number upstream of the shock in the frame of reference of the shock is given by

$$M_1' = \frac{\partial \bar{M}_1}{\partial x}\xi + \delta M_1 - \frac{1}{c_1}\dot{\xi} \tag{7}$$

with similar equations for all of the flow variables. It is useful to make a change of variables to use the independently propagating acoustic and entropy waves rather than perturbations in the flow variables. With the use of normalized wave amplitudes $\delta^\pm$ and δ^e given by

$$\begin{Bmatrix} 2\delta^+ \\ 2\delta^- \\ \delta^e \end{Bmatrix} = \begin{bmatrix} 1 & \gamma M & 0 \\ 1 & -\gamma M & 0 \\ -1/\gamma & 0 & 1 \end{bmatrix} \begin{Bmatrix} \dfrac{\delta p}{p} \\ \dfrac{\delta u}{u} \\ \dfrac{\delta \rho}{\rho} \end{Bmatrix} \tag{8}$$

then

$$\begin{Bmatrix} \left(\dfrac{\delta p}{p}\right) \\ \gamma M\left(\dfrac{\delta u}{u}\right) \\ \gamma\left(\dfrac{\delta \rho}{\rho}\right) \\ \gamma(\delta M) \end{Bmatrix} = \begin{bmatrix} 1 & 1 & 0 \\ 1 & -1 & 0 \\ 1 & 1 & \gamma \\ M^- & -M^+ & \gamma M/2 \end{bmatrix} \begin{Bmatrix} \delta^+ \\ \delta^- \\ \delta^e \end{Bmatrix} \tag{9}$$

where

$$M^\pm = 1 \pm [(\gamma-1)/2]M \tag{10}$$

Substituting the perturbations in each flow quantity, for example, Eqs. (6) and (7), into the shock equations (1) and (2) yields two equations that depend on the shock motion ξ and $\dot{\xi}$ and the perturbation amplitudes that can be represented by the waves $\delta_{1,2}^{\pm,e}$. These can then be solved for the shock motion, forced by the incoming waves and the amplitude of the downstream propagating wave δ_2^+ for $\xi = 0$. For convenience, the overbar will be dropped henceforth and nominal values of flow variables used unless otherwise indicated.

The shock motion satisfies the ODE,

$$(1/c_1)\dot{\xi} = -\alpha(\xi)\xi + \beta_2^-\delta_2^- + \beta_1^+\delta_1^+ + \beta_1^-\delta_1^- + \beta_1^e\delta_1^e \tag{11}$$

where

$$\alpha(\xi) = f_\alpha(M_1)\cdot\left(\frac{1}{A}\frac{\mathrm{d}A}{\mathrm{d}x}\right) \tag{12}$$

and $\beta_{1,2}^\pm$ are only a function of M_1. The variables $\delta_{1,2}^{\pm,e}$ capture the effects of upstream and downstream perturbations, including both disturbances and control. Equation (11) is of the same form as that derived previously,[5,6] but the dependence on M_1 differs slightly when the dynamics are derived for specified acoustic/entropy perturbations, rather than specified downstream pressure.

The functional form for f_α is always positive; thus, one immediately obtains that the shock is stable in the diverging section and unstable in the converging section. The response is also nonlinear because $\mathrm{d}A/\mathrm{d}x$ changes with the shock location. (In particular, it is zero at the throat.) This dependence of α on ξ introduces the nonlinear behavior seen in a latter figure.

Define

$$\mathcal{M} = 2M_1 + \frac{M_1^2+1}{M_1 M_2}$$

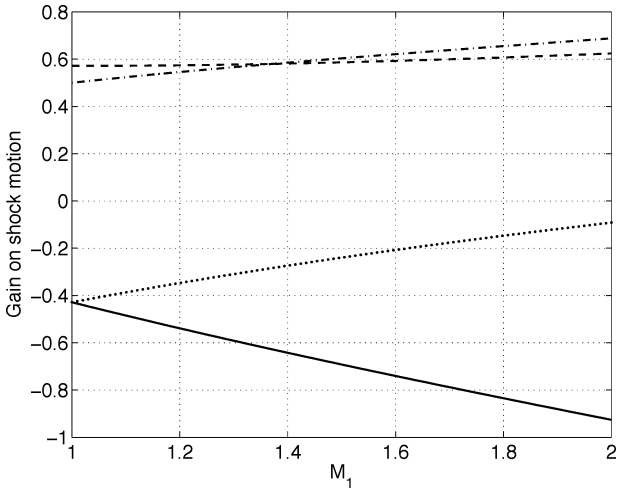

Fig. 2 Variation of gains with Mach number M_1 at the shock: ——, downstream acoustic wave β_2^-; – – –, upstream fast wave β_1^+; · · · ·, upstream slow wave β_1^-; and -·-·, entropy wave β_1^e.

Then

$$f_\alpha(M_1) = \frac{(\gamma-1)+(\gamma^2+1)M_1^2+\gamma(\gamma+1)\left(M_1^2/M_2\right)(u_2/u_1)}{(\gamma+1)\mathcal{M}} \tag{13}$$

$$\beta_2^- = -[(\gamma+1)/\gamma\mathcal{M}](p_2/p_1) \tag{14}$$

$$\beta_1^\pm = (1/\gamma\mathcal{M})\Big\{[(\gamma+1)/2](p_2/p_1)(1\mp M_2/M_1) \pm 2M_1^\mp(M_1+1/M_1M_2)\Big\} \tag{15}$$

$$\beta_1^e = (1/\mathcal{M})\left(M_1^2+1/M_2\right) \tag{16}$$

The gains β are plotted in Fig. 2. The influence of the fast upstream wave has an opposite sign to the remaining acoustic perturbations. Downstream perturbations have higher gain than slow upstream acoustic perturbations for $M_1 > 1$. For a weak shock these functions can be approximated by keeping terms only to first order in $M_1 - 1$:

$$\alpha(\xi, M_1) = \frac{\gamma}{4}(M_1+1)\left(\frac{1}{A}\frac{\mathrm{d}A}{\mathrm{d}x}\right) \tag{17}$$

$$\beta_2^-(M_1) = -\left[\frac{\gamma+1}{4\gamma}+(M_1-1)\frac{3\gamma-1}{4\gamma}\right] \tag{18}$$

$$\beta_1^+(M_1) = \frac{3-\gamma}{2\gamma} \tag{19}$$

$$\beta_1^-(M_1) = -\frac{\gamma+1}{4\gamma}(2-M_1) \tag{20}$$

$$\beta_1^e(M_1) = -\frac{1}{4}(M_1+1) \tag{21}$$

Close to the throat, the area variation can be approximated by

$$\frac{1}{A}\frac{\mathrm{d}A}{\mathrm{d}x} = \frac{1}{\ell^2}(d_{\mathrm{sh}}+\xi) \tag{22}$$

where the nominal shock location is defined by $d_{\mathrm{sh}} = x_{\mathrm{sh}} - x_{\mathrm{th}}$, with the throat at $\xi = -d_{\mathrm{sh}}$, and ℓ is the characteristic length. Define $\ell^* = \ell/f_\alpha^{1/2}$, $\xi^* = \xi/\ell^*$, $d^* = d_{\mathrm{sh}}/\ell^*$, $t^* = tc_1/\ell^*$ and δ^* as the sum over all disturbances of $\beta\delta$. Then a nondimensional form of the shock equation can be written as

$$\frac{\mathrm{d}\xi^*}{\mathrm{d}t^*} = -(d^*+\xi^*)\xi^* + \delta^* \tag{23}$$

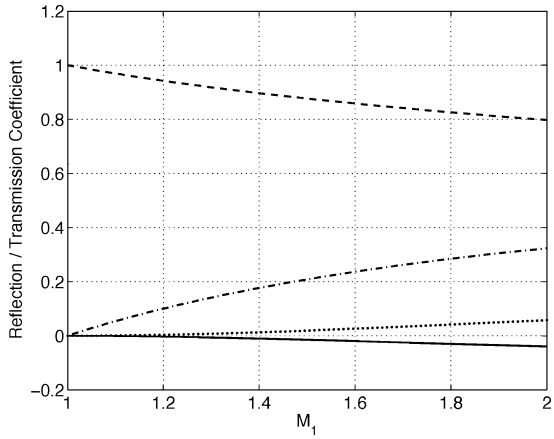

Fig. 3 Reflection and transmission coefficients for acoustic waves as a function of Mach number M_1 at the shock: ——, downstream acoustic wave; – – –, upstream fast wave; · · · ·, upstream slow wave; and -·-·, entropy wave.

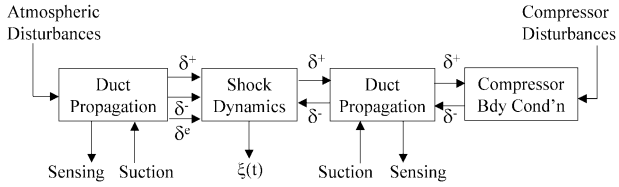

Fig. 4 Inlet system block diagram including coupling between shock dynamics, duct acoustic propagation, and downstream (compressor) boundary condition.

The amplitude of the downstream propagating acoustic wave δ_2^+ resulting from perturbations is represented using reflection and transmission coefficients σ_2^- and $\sigma_1^{\pm,e}$:

$$\delta_2^+ = \sigma_2^-\delta_2^- + \sigma_1^+\delta_1^+ + \sigma_1^-\delta_1^- + \sigma_1^e\delta_1^e \tag{24}$$

Define

$$\kappa = \frac{M_1^2+1}{2M_1^2M_2} \tag{25}$$

Then

$$\sigma_2^- = \frac{1-\kappa}{1+\kappa} \tag{26}$$

$$\sigma_1^\pm = \frac{\kappa \pm (M_2/M_1)\left[1+M_1^\mp(u_1/u_2-1)\right]}{1+\kappa} \tag{27}$$

$$\sigma_1^e = \frac{\gamma M_2/2(u_1/u_2-1)}{1+\kappa} \tag{28}$$

These coefficients are plotted in Fig. 3. For $M_1 \to 1$, then the fast upstream wave has a transmission coefficient of unity, whereas the remaining waves result only in shock motion and do not produce any downstream propagating wave. These results are consistent with previous results,[6,7] where the reflection coefficient was shown to be small and the transmission coefficient large (in terms of absolute, not relative amplitude).

IV. Inlet System

The model in the preceding section captures the dynamics of the shock. The overall inlet system, shown in Fig. 4, includes the creation and propagation of the acoustic waves caused by disturbances or control inputs and the downstream (compressor) boundary condition.

A. Disturbances

Atmospheric disturbances in general result in both acoustic and entropy disturbances. Assuming Kolmogorov turbulence, the energy

will decay with frequency as $f^{-5/3}$, with both acoustic waves having the same average amplitude.

Control of the inlet system can be achieved using variable suction or bleed at one or more locations. Suction is equivalent to an increase in area. Define the nondimensionalized control as $\mu = -\Delta A/A$, ($\mu \le 0$ is suction); then

$$\delta^+ = \frac{\gamma M_a}{2(M_a+1)}\mu \tag{29}$$

$$\delta^- = \frac{\gamma M_a}{2|M_a-1|}\mu \tag{30}$$

where M_a is the Mach number at the suction location. Both of the acoustic waves generated by suction are negative, both for suction in the supersonic and in the subsonic regions.

More generally, a one-dimensional disturbance source results in changes in mass, momentum, and energy; these can be transformed into the corresponding acoustic and entropy waves.[8]

B. Downstream Boundary Condition

The downstream boundary condition can have a significant influence on the inlet dynamics[2,3,9,10]; in particular, the dynamics are not well characterized by simulating with either constant pressure (reflection coefficient $R=-1$ and $\delta^+ = \delta^-$) or constant Mach number ($R = M^+/M^- > 1$). Detailed analysis[10] and experimentation[11] suggest that a realistic reflection coefficient is in the range from $R=+0.06$ to $+0.18$. In Refs. 10 and 11, it is also suggested that no significant reflection is generated from entropy waves.

In the spirit of low-order modeling, an alternative representation is presented based on the compressor characteristic,

$$\Delta p_c/\rho U^2 = \psi(u_c/U) = \psi(\phi) \tag{31}$$

which relates the pressure rise Δp_c across the compressor to the axial velocity u_c (normalized using the blade tip speed U). Changes in pressure and velocity are, therefore, related by the slope of the characteristic,

$$\delta(\Delta p_c)/p_c = -\gamma M_c^2 K(\delta u_c/u_c) \tag{32}$$

where

$$K = -\left(\frac{1}{\phi}\frac{\partial \psi}{\partial \phi}\right) \tag{33}$$

and $K>0$ for stable compressor operation. When both the reflected and transmitted acoustic waves are considered, the acoustic reflection coefficient is given by

$$\frac{\delta^-}{\delta^+} = \frac{\Pi \boldsymbol{M}(1+M_c) - (1+M_c')(1-M_cK)}{\Pi \boldsymbol{M}(1-M_c) + (1+M_c')(1+M_cK)} \tag{34}$$

where $\Pi = 1+\rho U^2\psi$ is the pressure ratio and $\boldsymbol{M} = M_c'/M_c$ is the ratio of Mach numbers across the stage. When it is assumed that there is constant axial velocity through the stage, then $\boldsymbol{M} \simeq \Pi^{(1-\gamma)/(2\gamma)}$. For small M_cK, $M_c \sim 0.5$, and $\Pi \sim 1.3$, this gives a reflection coefficient of $+0.2$, which increases with K, Π, or M_c.

C. Propagation

The duct acoustic propagation involves time delay, amplitude variation, and waveform variation due to the variation in wave speed with amplitude. Only the first two effects are considered.

The propagation time for each wave type to travel from x_i to x_j is given by

$$\tau^\pm = \int_{x_i}^{x_j} \frac{1}{c}\frac{1}{M\pm 1}\,\mathrm{d}x \tag{35}$$

$$\tau^e = \int_{x_i}^{x_j} \frac{1}{cM}\,\mathrm{d}x \tag{36}$$

For the area variation in Fig. 1, the characteristics for the three waves are shown in Fig. 5 for throat Mach number $M_{\text{th}} = 1.2$. Also shown

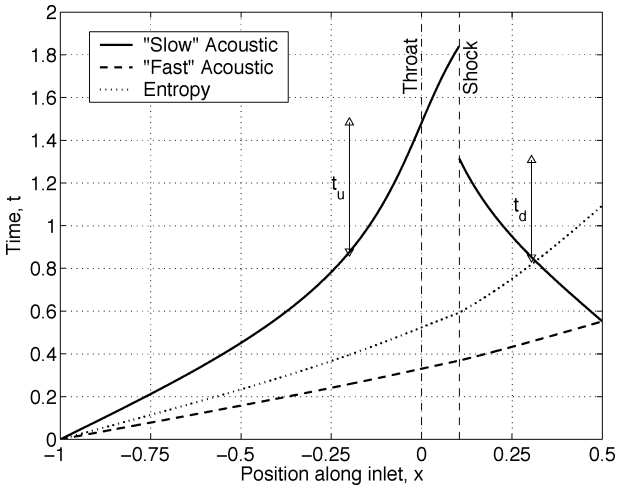

Fig. 5 Characteristics in x and t for the three independently traveling waves.

are the effective time delays for control, discussed in Sec. VI. For actuation 20% of the inlet-throat distance upstream of the throat or downstream of the shock location, the propagation time for the slow acoustic wave is shown by t_u or t_d, respectively. These are the effective time delays for control, discussed in Sec. VI.

Entropy is convected and does not change in amplitude. The acoustic waves, however, are affected by the area change. The Euler equations can be written as (e.g., Hirsch[12])

$$\left(\frac{\partial u}{\partial t} \pm \frac{1}{\rho c}\frac{\partial p}{\partial t}\right) + (u\pm c)\left(\frac{\partial u}{\partial x} \pm \frac{1}{\rho c}\frac{\partial p}{\partial x}\right) = \mp uc\frac{1}{A}\frac{\mathrm{d}A}{\mathrm{d}x} \tag{37}$$

plus a convection equation for entropy. Perturbing about the nominal solution and keeping terms to first order yields

$$\frac{1}{u\pm c}\frac{\partial w^\pm}{\partial t} + \frac{\partial w^\pm}{\partial x} = -\frac{1}{2(M\pm 1)^2}\left[\left(1\pm\frac{\gamma-1}{2}M^2\right)w^+ + \left(1\mp\frac{\gamma-1}{2}M^2\right)w^-\right]\left(\frac{1}{A}\frac{\mathrm{d}A}{\mathrm{d}x}\right) - \frac{\gamma c M^2(1\mp(M-1))}{4(M^2-1)}\delta^e\left(\frac{1}{A}\frac{\mathrm{d}A}{\mathrm{d}x}\right) \tag{38}$$

where $w^\pm = \pm c\delta^\pm$ are dimensional acoustic variables.

The left-hand side of Eq. (38) is the derivative along the characteristic $\mathrm{d}x/\mathrm{d}t = c^\pm = c(M\pm 1)$. Thus, isolated acoustic waves propagate according to

$$\left.\frac{1}{w^\pm}\frac{\mathrm{d}w^\pm}{\mathrm{d}x}\right|_{x=c^\pm t} = -\frac{1+[(\gamma-1)/2]M^2}{2(M\pm 1)^2}\left(\frac{1}{A}\frac{\mathrm{d}A}{\mathrm{d}x}\right) \tag{39}$$

$$\left.\frac{1}{w^\pm}\frac{\mathrm{d}w^\pm}{\mathrm{d}x}\right|_{x=c^\pm t} = -\frac{1}{2}\left(\frac{M\mp 1}{M\pm 1}\right)\frac{1}{M}\frac{\mathrm{d}M}{\mathrm{d}x} \tag{40}$$

where the second equation follows from Eq. (5). The change in amplitude in propagating from x_i (at M_i) to x_j is, therefore,

$$w_j^\pm \big/ w_i^\pm = [(M_i\pm 1)/(M_j\pm 1)](M_j/M_i)^{\frac{1}{2}} \tag{41}$$

The amplification of $\delta^\pm$ can be obtained from that of $w^\pm$ using the isentropic relationships for M and u,

$$\frac{\delta_j^\pm}{\delta_i^\pm} = \frac{M_i\pm 1}{M_j\pm 1}\left(\frac{M_j}{M_i}\right)^{\frac{1}{2}}\left\{\frac{1+[(\gamma-1)/2]M_j^2}{1+[(\gamma-1)/2]M_i^2}\right\}^{\frac{1}{2}} \tag{42}$$

This is plotted in Fig. 6 using the area variation of Fig. 1 for waves of unit amplitude at the inlet lip and unit δ^- at the downstream

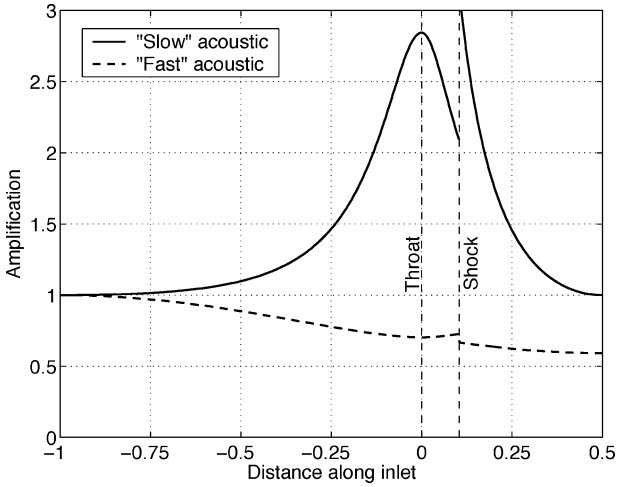

Fig. 6 Amplification of nondimensional acoustic waves $\delta^{\pm}$ due to area variation, for unit amplitude at the inlet lip and unit δ^{-} at the downstream boundary (slow acoustic wave propagates downstream ahead of the shock and upstream aft of the shock).

boundary. The extent of the amplification of the wave δ^{-} is strongly dependent on the throat Mach number.

The transfer function from any disturbance to any physical variable (other than the shock location) can be approximated by an expression of the form

$$H(s) = h^{+}e^{-s\tau^{+}} + h^{-}e^{-s\tau^{-}} + h^{e}e^{-s\tau^{e}} \tag{43}$$

where each coefficient h is the product of three coefficients

$$h = h_d h_p h_s \tag{44}$$

that give the amplitude of the corresponding wave h_d for the disturbance [for example, Eq. (30)], the variation in amplitude h_p due to propagation from disturbance to sensor location [Eq. (42)], and the contribution of the corresponding wave to the physical variable h_s [Eq. (9)]. Large-amplitude disturbances distort; this nonlinearity cannot be captured in transfer function form.

As acoustic waves propagate through a nonuniform area, small amplitude acoustic waves of the other type are also generated; these can also be obtained from Eq. (38). As an entropy wave propagates, both acoustic waves are generated. For simplicity, these effects are ignored in the subsequent analysis of actuator authority; the effect on the transfer function could be captured by including additional integral terms in Eq. (43).

V. System Dynamics

Several observations about the uncontrolled system dynamics can be made based on the modeling in the preceding sections. The key questions pertinent to control system design are the open-loop response and the relative authority of different disturbances or control inputs.

A. Frequency Response

The shock motion was simulated in MATLAB® by integrating Eq. (23) using a variable time-step explicit 4th/5th order Runge–Kutta formula. The shock motion is nonlinear, as shown in Fig. 7; exciting the shock with a sinusoidal disturbance (illustrative, not realistic) generates a slow movement of the shock toward the throat, with the possibility of eventual unstart (similar to Fig. 4 in Ref. 13). Thus, one cannot predict the maximum shock motion by using the value of α at $\xi = 0$.

The shock responds more to low-frequency disturbances than high frequency, with zero-frequency disturbances being the most destabilizing. For a disturbance pulse that is short compared to the time constant $1/\alpha$, only the total impulse of the pulse matters and not the detailed shape. For a given inlet geometry $A(x)$, increasing the

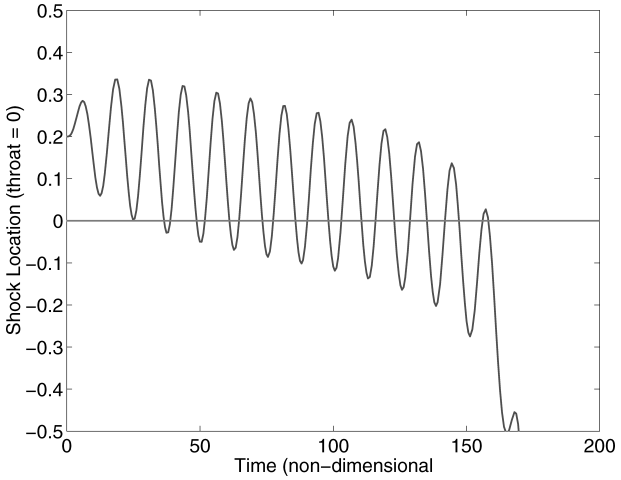

Fig. 7 Nonlinear shock response to a sinusoidal disturbance.

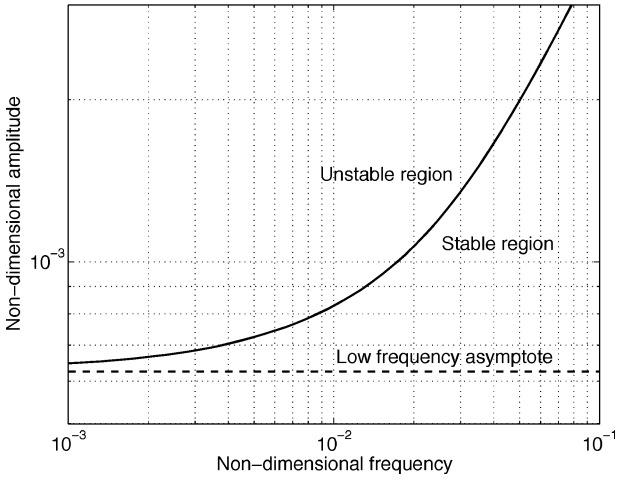

Fig. 8 Computed stability boundary as a function of nondimensional forcing amplitude and frequency; nondimensional nominal shock location is 0.05.

throat Mach number does not significantly improve shock stability. The largest disturbance that can be tolerated without instability can be obtained by setting $\dot{\xi} = 0$ in Eq. (11) and setting $\beta\delta$ equal to the maximum value of $\alpha(\xi)\xi$. With use of the area variation in Eq. (22), then for small M_1 the maximum downstream disturbance (at the shock location) that can be tolerated is

$$\delta_M = [\gamma^2/2(\gamma+1)](d_{\mathrm{sh}}/\ell)^2 \tag{45}$$

The largest compressor disturbance that can be tolerated follows from Eq. (42). The largest stable (non-dimensional) disturbance that can be tolerated as a function of frequency is shown in Fig. 8.

B. Disturbance and Actuator Authority

Upstream of the throat, fast and slow acoustic disturbances of equal amplitude at x_i propagating to x_j satisfy

$$\frac{\delta_j^{-}}{\delta_j^{+}} = \frac{(M_j+1)}{(M_j-1)}\frac{(M_i-1)}{(M_i+1)} \tag{46}$$

Hence, $h_p^{-} > h_p^{+}$ in Eq. (44); for $M_\infty = 2.2$ and $M_{\mathrm{th}} = 1.2$, then $h_p^{-}/h_p^{+} > 4$. For the throat Mach number, $h_s^{-} > h_s^{+}$, whereas for the shock the gain for fast waves is not sufficiently larger than the gain for slow waves to offset these effects. Therefore, for small M_{th} and M_{sh}, perturbations at either the throat or the shock due to upstream (atmospheric) disturbances are dominated by slow acoustic waves.

For suction upstream of the throat, δ^{-} is negative and acts to stabilize both M_{th} and the shock location, whereas the fast wave

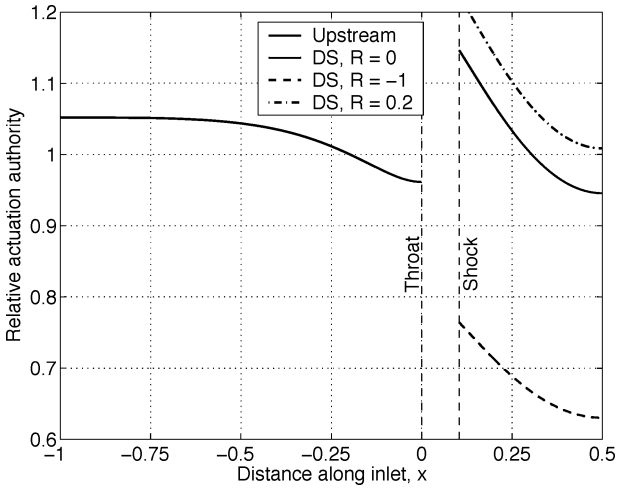

Fig. 9 Relative actuation authority; amplitude of resulting wave δ^- at throat or shock normalized by the authority at 20% of the inlet-throat distance upstream of the throat or downstream of shock, respectively.

that is produced destabilizes both M_{th} and the shock. However, from Eqs. (29), (30), and (42), the relative amplitude of fast and slow waves at a point x_j downstream of the suction is

$$\delta_j^- \big/ \delta_j^+ = (M_j + 1)/(M_j - 1) \tag{47}$$

Thus for M_{th} or $M_{\text{sh}} \simeq 1.2$, the slow wave produced by actuation is more than 10 times as large as the fast wave, and the latter can be ignored. With this approximation, the variation in control authority with forcing location, plotted in Fig. 9 (for $x < 0$), is a function only of the Mach number at the actuator location M_a:

$$\left\{ \frac{M_a}{1 + [(\gamma - 1)/2]M_a^2} \right\}^{\frac{1}{2}} \tag{48}$$

The overall amplification is not strongly sensitive to injection location unless the Mach number at the injection location is very close to unity.

Suction downstream of the shock also acts to stabilize the shock, but the response includes contributions from both the upstream propagating acoustic wave and the downstream wave that reflects off of the compressor (or downstream) boundary condition. The latter term is obtained from Eqs. (29) and (30) and the net change in amplitude due to propagation of the wave traveling rightward from the actuator to the boundary condition and returning leftward to the actuator location again, using Eq. (42). The variation in (low-frequency) control authority with forcing location depends on the reflection coefficient R and the exit Mach number at the compressor face M_c:

$$\left\{ \frac{M_a}{1 + [(\gamma - 1)/2]M_a^2} \right\}^{\frac{1}{2}} \cdot \left(1 + R \frac{1 - M_c}{1 + M_c} \right) \tag{49}$$

This is plotted in Fig. 9 (for $x > 0$) for $M_c = 0.5$ and $R = 0$, $R = -1$ (constant pressure), and $R = 0.2$ (typical compressor boundary condition). The optimal forcing location does not depend on R; however, the resulting authority does. For the true compressor, $R > 0$ and the impact of the boundary condition is beneficial, whereas for a constant pressure boundary condition the term is detrimental.

VI. Control

A. Approach

The inlet system can unstart either due to the existing shock being perturbed past the inlet throat, due to either upstream or downstream disturbances, or by the throat Mach number dropping below unity. The latter results in a new (unstable) shock being created immediately upstream of the throat. Because of the propagation time delays inherent in the system, feedback control bandwidth is limited. Each of these unstart mechanisms, therefore, requires both feedforward and feedback control. Analysis of shock control requires some understanding of throat Mach number control because this influences the disturbances that affect the shock.

Feedforward control requires an estimate of the disturbances. Rather than independent measurements of p, ρ, and u, the different wave types can be extracted using differential pressure measurements (see the Appendix). Feedback control ideally requires direct measurement of the quantities of interest, throat Mach number M_{th} and shock location ξ. The latter would involve either a distributed array of sensors or a model-based estimation from a subset of sensors. An alternative is to have one or more discrete sensors at locations ξ_i from which one can establish whether $\xi > \xi_i$; this strategy is verified in Sec. VI.C.

Recall that the influence on throat Mach number from upstream bleed is primarily through the propagation of the slow acoustic wave. Therefore, fast acoustic and entropy disturbances can only be controlled by generating slow acoustic waves to cancel their effect. For most actuator/sensor placements, the time delay means that these disturbances can only be controlled with relatively low bandwidth. With suction 20% of the distance upstream from the throat toward the inlet, the propagation time (t_u in Fig. 5) for the slow acoustic wave to reach the throat is larger than the time for a fast acoustic wave to propagate from the inlet lip to the throat for $M_{\text{th}} = 1.2$. Differential pressure measurements do not provide low-bandwidth information about separate wave types; hence, the use of feedforward information (within the inlet) for control of fast and entropy disturbances is of marginal value. To control throat Mach number, then, the steps are 1) estimate slow acoustic disturbances and 2) create a canceling wave using a simple time-delay controller, with 3) low-bandwidth feedback control of M_{th} to compensate both for feedforward errors and fast acoustic and entropy disturbances. However, this feedback control of the throat Mach number will result in residual fast and slow acoustic disturbances that impact the shock location.

The shock location can be controlled using suction either upstream or downstream of the shock. (Although upstream bleed may already be used to control M_{th}, suction stabilizes both M_{th} and ξ, and hence, the same actuator could be used for both.) For actuation the same distance from the shock, the time delay for the slow acoustic wave is comparable, whereas the authority is higher for downstream suction ($\beta_2^- > \beta_1^-$). The fast wave generated by upstream suction influences the shock with the opposite sign, whereas with $R > 0$ the fast wave generated by downstream suction increases authority. Thus, downstream suction is preferable.

Feedforward control for shock motion requires a differential measurement to identify disturbances propagating from the compressor and potentially processing of the upstream information to obtain the residual waves that will result from feedback control of M_{th}. Depending on the Mach number at the shock, the time delay for downstream control (t_d in Fig. 5) may be larger than the propagation time for the fast acoustic wave from the inlet lip to the shock. Thus, any feedforward information from upstream of the shock may not be of sufficient benefit to warrant the additional complexity.

B. Authority and Bandwidth

For control of the throat Mach number, the required actuator authority can be roughly estimated by considering only the slow acoustic disturbance and using the amplification of that wave between the inlet lip and the actuator location [Eq. (42)] and the amplitude of the wave generated [Eq. (30)]. The bandwidth required is a function of the atmospheric disturbance model; sufficient (feedforward) bandwidth is required so that the cumulative impact of uncontrolled disturbances on throat Mach number [from Eqs. (42) and (9)] is insufficient to perturb the throat below Mach one. Given an atmospheric disturbance model, this calculation is straightforward.

For control of the shock motion, assume for simplicity that the residual destabilizing disturbances left by the upstream control of throat Mach number are smaller than the downstream disturbances from the compressor. Although not required, this assumption is reasonable if the upstream control cancels any slow acoustic

disturbance and responds to fast or entropy waves with a slow wave that stabilizes both M_{th} and ξ. The required actuator authority μ_M can be directly estimated from the maximum disturbance amplitude as $\mu_M > \delta_M$, where both δ_M and μ_M are expressed as the amplitude of the wave δ_2^- that arrives at the shock due to the maximum disturbance or control, respectively. From Eqs. (30) and (42), the suction required is related to the pressure perturbation from the compressor.

The minimum time delay for control of the shock, including actuator bandwidth, computational delay, and propagation delay, can also be obtained. Assume that α is small compared to the disturbances that are expected. The worst-case disturbance is a step change to the maximum value. The shock, therefore, moves at $\dot{\xi} \simeq \beta_d^- \delta_M c_1$. If $\mu_M = \delta_M$, then the maximum time lag τ_M for applying μ_M is the time it takes the shock to move from its nominal location x_{sh} to the throat, or

$$\tau_M < (1/c_1 \beta \delta_M) d_{\text{sh}} \tag{50}$$

This estimate is conservative and can be refined by including the effects of α. If the actuator has greater authority, then some motion of the shock past the throat is possible, and greater time delay can be tolerated. The estimate is based on an instantaneous step change in the disturbance, and lower disturbance bandwidth will also permit higher time lag. If the time lag is dominated by propagation, then one can obtain a constraint on the actuator injection location, $d_a = x_a - x_{\text{th}}$, to satisfy the time delay, as

$$d_a/d_{\text{sh}} < (1 - M_2)/\beta \delta_M \tag{51}$$

where the variation in Mach number has been ignored for simplicity.

C. Control Law Analysis

Feedback control of throat Mach number is straightforward given a direct measurement of performance, M_{th}. However, direct measurement of the shock location ξ requires an array of sensors. The following analysis, therefore, compares this case against feedback control using only a single sensor. Both the actuator saturation and the time delay must be taken into account in the design of the control over the shock location.

Consider two control laws; the first is proportional, whereas the second assumes only a single feedback sensor:

$$\mu_a(\xi) = \begin{cases} 0 & : \quad \xi > 0 \\ -K\xi & : \quad 0 > \xi > \xi_0^a \\ \mu_M & : \quad \xi < \xi_0^a \end{cases} \tag{52}$$

$$\mu_b(\xi) = \begin{cases} 0 & : \quad \xi > \xi_0^b \\ \mu_M & : \quad \xi < \xi_0^b \end{cases} \tag{53}$$

For $\mu_M = \delta_M$ and $\tau = \tau_M/1.5$, the proportional gain in $\mu_a(\xi)$ required for (marginal) stability is $K = 1.5\mu_M/d_{\text{sh}}$; this applies between the nominal shock location ($\xi = 0$) and saturation at $\xi = \xi_0^a = d_{\text{sh}}/1.5$. The design parameter ξ_0^b in $\mu_b(\xi)$ can be chosen based on the ratio between the actual time delay τ and the maximum value τ_M derived earlier, $\xi_0^b = (1 - \tau/\tau_M)d_{\text{sh}}$. For $\tau = \tau_M/1.5$, the simple control μ_b turns on when the shock moves one-third of the distance toward the throat, whereas the smooth control μ_a saturates at two-thirds the distance.

The simulated control behavior is shown in Fig. 10 using a fixed time-step forward Euler numerical integration that allows straightforward coding of the discontinuous time-delayed control law. Numerical accuracy is achieved by using a sufficiently small time step. The control time delay is $\tau = \tau_M/1.5$, and the disturbance amplitude is equal to the maximum control, $\mu_M = \delta_M = 0.05$. This disturbance would lead to instability without control. The response is shown for two cycles of disturbance after the system has reached steady state. Both control laws stabilize the system, with the first control law $\mu_a(\xi)$ resulting in a smoother response. Any actuator dynamics would result in some smoothing of the response shown for the simple control law $\mu_b(\xi)$. The ultimate performance metric

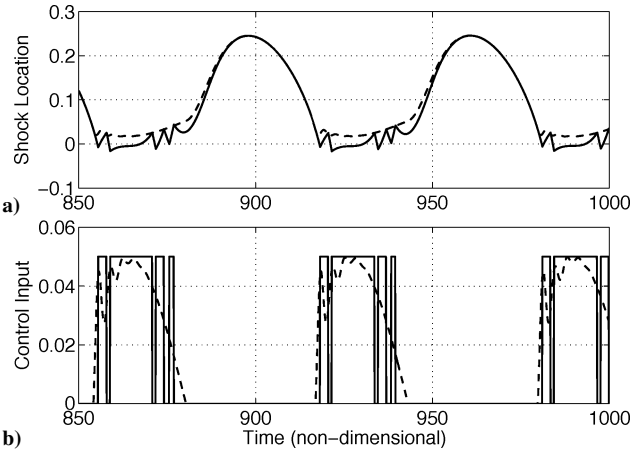

Fig. 10 Comparison of control response to 5% perturbation: a) shock location and b) control: – – –, smooth control law μ_a and ——, simple control law μ_b.

is to retain stability with minimum bleed requirements. Based on this metric, the smooth control law slightly outperforms the simple control law for the worst-case disturbance shown, but is worse for smaller disturbances. For sufficiently small disturbances, the simple controller does not respond at all.

A single sensor and a simple control law are adequate for stabilizing the shock. Any performance improvement of the smooth controller would likely be outweighed by the extra complexity. If necessary, a second sensor may provide an adequate compromise between the simple and smooth controllers.

VII. Conclusions

Active stabilization of a weak shock in a near-isentropic inlet would prevent unstart and enable lower loss supersonic inlets to be designed. Control is required both of the nominal shock and also to prevent the throat Mach number from dropping below unity because either mechanism can lead to unstart. A simple model involving a single nonlinear ODE captures the relevant shock dynamics for both upstream and downstream disturbances, as well as the acoustic reflection and transmission properties of the shock. The variation in amplitude of acoustic waves propagating through the inlet is captured via perturbation of the Euler equations. This low-order model of the inlet/shock system dynamics is used to parametrically assess actuator and sensor selection, actuator authority and bandwidth requirements, and to compare different control strategies. For control of the shock, downstream suction is preferable to upstream suction. A simple feedback control law that relies on a single sensor to determine when the shock is upstream of a critical location is sufficient to stabilize the system.

The actual inlet/shock dynamics involve viscous and two- and three-dimensional effects, and therefore, the conclusions based on the low-order model herein should be considered as initial guidance only. Nonetheless, this model allows general conclusions to be made that would be difficult or impossible to obtain with a complex computational simulation.

Appendix: Disturbance Sensing

Both the upstream and downstream feedforward controllers require knowledge of each of the independently traveling waves. Rather than sense these using independent measurements of p, u, and ρ (or other independent variables), the overall system is simpler if one can extract the wave amplitudes from pressure measurements. This can be done by relying on the difference in propagation speeds between different pressure sensors. For two waves traveling at $c_1 \neq c_2$, then $y(t) = \tilde{p}(x, t) - g\tilde{p}(x - \Delta x, t - \tau_i)$ can be made independent of wave type i by choosing $\tau_i = (\Delta x)/c_i$ [or from Eq. (35)], where $\tilde{p}$ is the deviation from nominal pressure. With varying duct area, g accounts for amplification and can be obtained

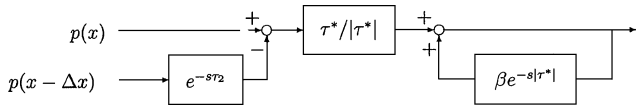

Fig. A1 Block diagram for uniform-gain wave sensor based on differential pressure measurements.

from Eq. (42). The resulting signal $y(t)$ measures the remaining wave type $j \neq i$ with frequency response

$$H_s(s) = 1 - e^{-s\tau^*} \tag{A1}$$

where $\tau^* = \tau_i - \tau_j$. A more uniform frequency response can be obtained with a positive feedback loop,

$$z(t) = \text{sgn}(\tau^*)y(t) + \beta z(t - |\tau^*|) \tag{A2}$$

with $\beta < 1$ for stability. This is shown schematically in Fig. A1. Note that the output is always zero at zero frequency. For $\tau^* < 0$ ($\tau^* > 0$), then $z(t)$ approximates the wave amplitude at the first (second) sensor location. Differential pressure measurements are subtracted with an appropriate time delay, and fed through a positive feedback loop to recover approximately constant gain at nonzero frequencies.

The disturbance sensing can be extended to separation of three wave types using three pressure measurements. For simplicity, assume both separations are Δx, then

$$y(t) = \tilde{p}(x_0, t) - \tilde{p}(x_0 - \Delta x, t - \tau_i) + \tilde{p}(x_0 - \Delta x, t - \tau_j) - \tilde{p}(x_0 - 2\Delta x, t - \tau_i - \tau_j) \tag{A3}$$

provides a measurement of a wave traveling at speed $c_k \neq c_i, c_k \neq c_j$. The filter

$$(1 - e^{-s\tau_i}e^{+s\tau_k})^{-1}(1 - e^{-s\tau_j}e^{+s\tau_k})^{-1} \tag{A4}$$

that provides a reasonably uniform frequency response can be built as a series feedback network with each component as before.

The magnitude of the sensor response at low frequency is determined by the difference in propagation time for the different waves. At low frequencies, the feedback amplification may lead to excessive sensor noise. For example, at frequency ω the amplification k in distinguishing slow acoustic waves from entropy is a function of the Mach number M_s at the sensor location,

$$\omega k \simeq M_s(M_s - 1)(c/\Delta x) \tag{A5}$$

Acknowledgments

A one-dimensional Euler code provided by James Paduano and Ali Merchant at the Massachusetts Institute of Technology was invaluable in validating the low-order model derived herein. Timothy Colonius at the California Institute of Technology assisted with the model development.

References

[1]Mayer, D. W., and Paynter, G. C., "Prediction of Supersonic Inlet Unstart Caused by Freestream Disturbances," *AIAA Journal*, Vol. 33, No. 2, 1995, pp. 266–275.

[2]Numbers, K., and Hamed, A., "Conservation Coupling Technique for Dynamic Inlet-Engine Analyses," *Journal of Propulsion and Power*, Vol. 19, No. 3, 2003, pp. 444–455.

[3]Giannola, P., Haas, M., Cole, G., and Melcher, K., "Modeling the Dynamics of Supersonic Inlet/Gas-Turbine Engine Systems for Large-Amplitude High-Frequency Disturbances," AIAA Paper 2000-3594, July 2000.

[4]Zha, G.-C., Knight, D., and Smith, D., "Investigations of High-Speed Civil Transport Inlet Unstart at Angle of Attack," *Journal of Aircraft*, Vol. 35, No. 6, 1998, pp. 851–856.

[5]Hurrell, H. G., "Analysis of Shock Motion in Ducts During Disturbances in Downstream Pressure," NACA TN 4090, Sept. 1957.

[6]Culick, F. E. C., and Rogers, T., "Response of Normal Shocks in Diffusers," *AIAA Journal*, Vol. 21, No. 10, 1983, pp. 1382–1390.

[7]Yang, V., and Culick, F. E. C., "Analysis of Unsteady Inviscid Diffuser Flow with a Shock Wave," *Journal of Propulsion and Power*, Vol. 1, No. 3, 1985, pp. 222–228.

[8]Sajben, M., Cole, G. L., and Slater, J. W., "Acoustic and Entropy Pulses Created in Duct Flows by Rapid Local Events," *AIAA Journal*, Vol. 41, No. 3, 2003, pp. 538–542.

[9]Slater, J. W., and Paynter, G. C., "Implementation of a Compressor Face Boundary Condition Based on Small Disturbances," *Journal of Turbomachinery*, Vol. 123, April 2001, pp. 386–391.

[10]Sajben, M., and Said, H., "Acoustic-Wave/Blade-Row Interactions Establish Boundary Conditions for Unsteady Inlet Flows," *Journal of Propulsion and Power*, Vol. 17, No. 5, 2001, pp. 1090–1099.

[11]Opalski, A. B., and Sajben, M., "Inlet/Compressor System Response to Short-Duration Acoustic Disturbances," *Journal of Propulsion and Power*, Vol. 18, No. 4, 2002, pp. 922–932.

[12]Hirsch, C., *Numerical Computation of Internal and External Flows*, Vol. 2, Wiley New York, 1990, Chap. 16.

[13]Biedron, R. T., and Adamson, T. C., "Unsteady Flow in a Supercritical Supersonic Diffuser," *AIAA Journal*, Vol. 26, No. 11, 1988, pp. 1336–1345.